Heat-Sink Structural Design Concepts for a Hypersonic Research Airplane

Allan H. Taylor*
Vought Corporation, Hampton Technical Center, Hampton, Va.
and
L. Robert Jackson†
NASA Langley Research Center, Hampton, Va.

Hypersonic research aircraft design requires careful consideration of thermal stresses. This paper relates some of the problems in a heat-sink structural design that can be avoided by appropriate selection of design options, including material selection, design concepts, and load paths. Data on several thermal loading conditions are presented on various conventional designs including bulkheads, longerons, fittings, and frames. Results indicate that conventional designs are inadequate and that acceptable designs are possible by incorporating innovative design practices. These include nonintegral pressure compartments, ball-jointed links to distribute applied loads without restraining the thermal expansion, and material selections based on thermal compatibility.

Nomenclature

E = Young's modulus of elasticity
g = acceleration of gravity
K = restraining factor
k = thermal conductivity
Δl = change in length
L = length
M = Mach number
Q = dynamic pressure
ΔT = temperature difference
α = coefficient of thermal expansion
σ = stress

Introduction

As part of a continuing joint NASA/USAF study of a hypersonic research aircraft,[1] an in-house design and analysis is being performed for an advanced heat-sink structure suited to the research airplane mission. This paper addresses some thermostructural problems that are encountered in the design of a heat-sink structure for a hypersonic research aircraft. In this application, unavoidable thermal stresses in the structural frames are induced because the exterior surface of the airplane is exposed to high heating rates causing the skin temperature to rise more rapidly than the inner frame elements. Trajectory and heat-transfer analysis indicate that a 650°F temperature difference can exist in these frames. This ΔT is sufficient to fail a conventional structure with no other superimposed loads.

The structural analysis of multiply redundant monocoque structures is tedious at best. The addition of transient thermal loading parameters to the already complex analysis leaves the engineer no choice but to rely on computer-aided solutions to the structural design.

This paper presents some design and analysis techniques used to successfully satisfy the structural requirements for a heat-sink structure.

Received March 17, 1977; presented as Paper 77-392 at the AIAA/ASME 18th Structures, Structural Dynamics and Materials Conference, San Diego, Calif., March 21-23, 1977; revision received Dec. 16, 1977.

Index categories: Structural Design; Thermal Stress.

*Project Engineer. Member AIAA.
†Aerospace Engineer, Hypersonic Aerodynamics Branch, HSAD. Member AIAA.

Thermal Stress

Metallic structural materials exhibit positive coefficients of thermal expansion, α, i.e., they increase in volume with increasing temperature. Materials that are heated at very low and uniform heating rates and are not constrained in their growth, generate no thermal stresses; the heated component merely increases in size. However, when the material is prevented from growing by infinitely rigid external restraints, a stress σ of magnitude $E\alpha\Delta T$ will be generated. It should be noted that the area is not a variable, and that the stress is not directly influenced by the addition or subtraction of material. Only the total force exerted on the constraint by the heated component is changed by changing the area.

The independent variables in the thermal stress calculations are the modulus of elasticity, the coefficient of thermal expansion, and the temperature differential. To compute realistic thermal stresses, a fourth variable must be added. The infinitely rigid restraint previously mentioned is not possible, so a restraining factor K must be added to the thermal stress equation yielding $\sigma = KE\alpha\Delta T$. Deflections caused by the applied thermal load will reduce the stress in the thermally strained member by a factor K by allowing some thermal expansion. Thus, the thermal stress in a structural member will be a maximum corresponding to $K = 1$, for a fully restrained member and will be nonexistent ($K = 0$) for an unrestrained member.

This explanation of thermal stresses is fundamental to understanding thermal-structural design. Actually, thermal stresses may be categorized as stresses caused either by external restraints or stresses caused by internal restraints. The stresses in the first category have been previously discussed. Those in the second category are the result of regions of the structure having different temperatures, different stiffnesses, or different expansion coefficients. Under these conditions, the member may restrain itself thus producing thermal stresses.

Examples of these categories are depicted in Fig. 1. All members shown are aluminum bars of constant thickness heated to 500°F. They have no residual stress at the 0°F initial temperature. In Fig.1a an unrestrained cantilevered aluminum bar is heated to 500°F at a very low heating rate. In this case, no stresses are present, and the K factor is equal to zero. The same heating is applied to the same bar in Fig. 1b. However, in this case, the bar is constrained from expanding, i.e., $K = 1$. In this instance, the thermal stress will equal the

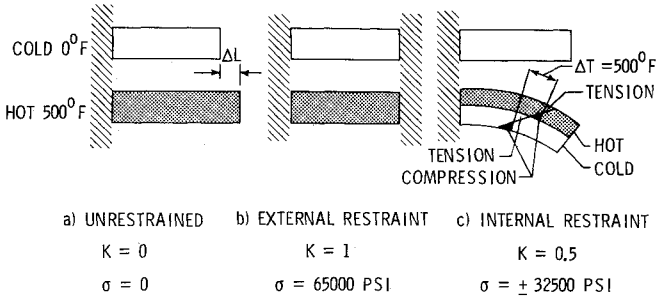

Fig. 1 Comparison of thermal stress categories.

full $E\alpha\Delta T$ value shown providing the stresses remain within the elastic range of the material. In the third case, Fig. 1c, only one-half the thickness of the bar is raised to the 500°F temperature, and the end is not constrained. No external loads or moments are applied, but this stepped temperature profile causes an internal constraint.

The hot half of the bar attempts to expand while the cold lower half resists this growth. At the midplane, the thermal interface, the expanding surface is attempting to stretch the cold lower half of the bar forcing the hot interface into compression and the cold lower interface into tension. These interface shear forces are eccentric to the upper and lower bar halves causing equal and opposite bending moments within the bar. The bending places the extreme fibers for the top surface in tension and the lower surface in compression, resulting in equal and opposite stresses in each bar half.

Research Airplane Configuration

The configuration definition for the aircraft designated as the National Hypersonic Flight Research Facility (NHFRF)[1] is currently under study by a joint NASA/USAF team. One of the early candidate configurations shown in Fig. 2 was used in this structural study. This aircraft is 50 ft long, has a maximum body depth of 7.25 ft and a 24.2-ft wingspan. It is designed to be air-launched from a B-52 in a manner similar to the X-15 and other research airplanes. The 60,000-lb launch weight along with the wingspan and body depth are constrained by the B-52 launch vehicle.

The primary structure consists of a relatively thick heat-sink skin designed not to exceed 600°F.[2] Ring frames on 20-in. centers are 3 in. deep on the top and sides of the aircraft and 4 in. deep on the bottom. The skin thickness is sized for the local nominal heat load and, for the majority of the surface, requires no additional stiffness to resist buckling.

Heat-Sink Material

Lockalloy (Be-38Al), a state-of-the-art beryllium-aluminum alloy was selected for the heat-sink skin. This selection was based on the unique properties of the Lockalloy material. It has a specific heat of 0.45 Btu/lb°F, which is almost twice the value for aluminum and four times that of the nickel alloys. Similarly, the conductivity k of 1440 Btu/in./h-ft²°F of this material is much higher than other heat-sink materials. It has a specific stiffness and strength superior to both aluminum and Inconel-X.[2]

The Lockalloy material is also readily adaptable to conventional fabrication techniques. It can be welded, drilled, cut, formed, and fastened with no exotic tooling requirements. Although this material has been available for over 10 years, its unique properties have been exploited only recently in a large-scale aircraft structural application for the YF-12A ventral fin. Further characterization of the Lockalloy material can be obtained in Ref. 3.

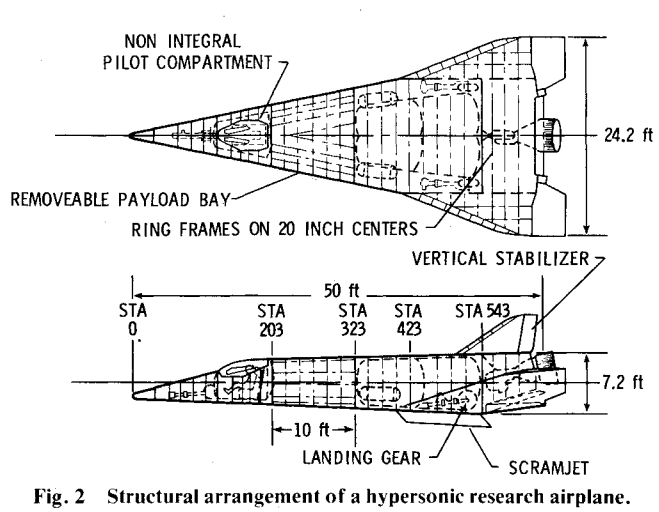

Fig. 2 Structural arrangement of a hypersonic research airplane.

Loads

Loads and design criteria were established to represent proposed flight missions.[2] The nominal mission selected for this study consists of a B-52 air-launch at a 45,000-ft altitude and Mach 0.85 followed by a 2-min rocket-powered flight to approximately an 100,000 ft altitude and Mach 7. Rocket-powered cruise is sustained for 60 s before an unpowered glide to landing. Two limit missions were investigated to establish transient time-temperature histories for the structure. Both missions achieve Mach 9 burnout, one at a peak 1000 psf dynamic pressure, low Q, while the second has a higher dynamic pressure of 1250 fps, which is held by a rapid descent for 60 s producing the limit heat load, designated as high Q.

Figure 3 summarizes the numerous load cases analyzed. The temperature profiles across a typical frame for each limit condition are also shown. A vent pressure and 4g maneuver load are combined with the first limit case while only 1g and the vent pressure are applied to the second, high dynamic pressure limit case. Additionally, conventional loads, such as landing, B-52 pylon attachment, thrust, and pullup after launch, were also analyzed. The local skin thickness is governed by the heat load from a nominal Mach 7 trajectory. The skin thickness is proportioned to the local heat load to provide uniform external temperatures of 600°F. This skin thickness is then retained throughout the analysis. The limit load cases produce maximum skin temperatures of approximately 600 and 750°F, respectively. The rationale for these loads is discussed in more detail in Ref. 2.

Heat-Sink Structure

Figure 4 represents the typical heat-sink structure. Removable heat-sink skin panels are bolted to a redundant frame structure consisting of circumferential frames and

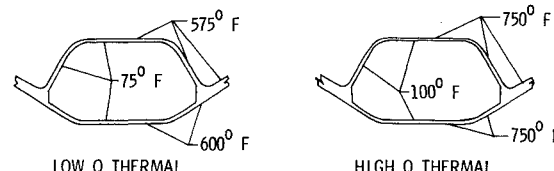

CASE		
1	LOW Q THERMAL 1	600° F LOWER, 575° F SIDES, 75° F INSIDE
2	VENT PRESSURE	1 PSI VACUUM INSIDE FUSELAGE
3	AERODYNAMIC PRESSURE	1.095 PSI ON LOWER SURFACE AND WING
4	4g INERTIA LOAD	4 G'S + AIR LOADS AND REACTIONS + VENT
5	LOW Q LIMIT SET	4 G + LIMIT THERMAL 1
6	LOW Q ULTIMATE SET	6 G + LIMIT THERMAL 1
7	1g INERTIA LOAD	WEIGHT AND BALANCE
8	HIGH Q THERMAL 2	750° F EXTERIOR 100° F INSIDE
9	HIGH Q LIMIT SET	1 G + LIMIT THERMAL 2
10	HIGH Q ULTIMATE SET	1.5 G + LIMIT THERMAL 2
11	PYLON LOADS	-2 G CAPTIVE FLIGHT ON FITTINGS
12	PULLUP AT LAUNCH	2.5 G WITH PROPELLANTS AND THRUST
13	LANDING LOADS	2 G ON LANDING GEAR
14	TEMPERATURE DIFFERENCE	LIMIT THERMAL 2 WITH COLD AREA SCRAMJET

Fig. 3 Summary of typical hypersonic research aircraft loads and design conditions.

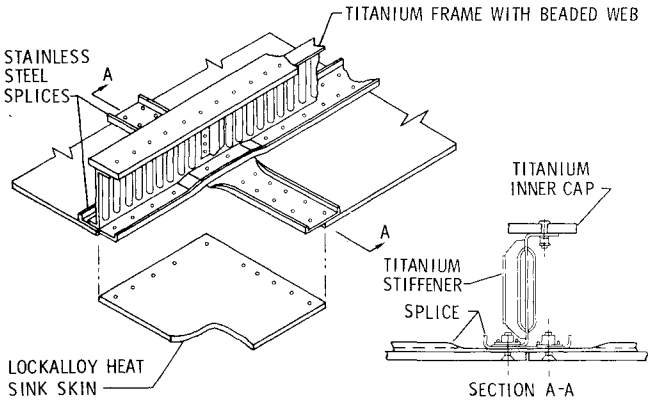

Fig. 4 Fuselage heat-sink structural design.

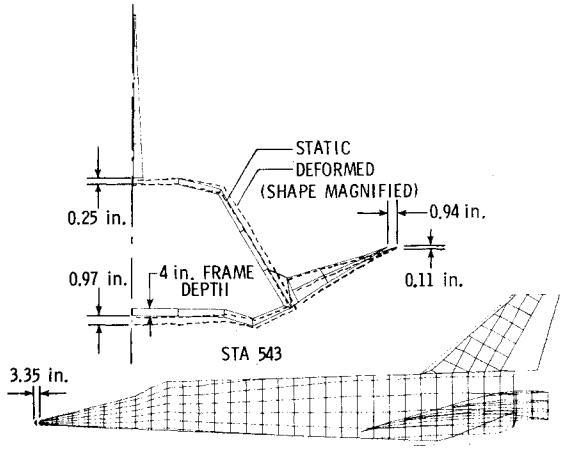

Fig. 5 Thermal growth due to 600°F heating.

longitudinal splices. Material selection for these structural components is fundamental to a successful design. Lockalloy, due to its unique properties, was selected for the heat-sink skin. The remaining structure was then selected for compatibility with these heat-sink skins. Stainless steel was utilized for the outer frame caps and longitudinal splices because its coefficient of thermal expansion is approximately the same as Lockalloy, 9.2 and 9.4×10^{-6} in./in./°F, respectively. The circumferential frame webs and inner caps were titanium due to its high strength and low elastic modulus (relative to Lockalloy) to minimize thermal stresses. The rationale and analyses employed in selecting these materials over other candidates will be discussed in subsequent sections.

Structural Analysis

A finite-element analysis was undertaken using the SPAR (Structural Performance and Resize) system of computer programs.[4] The complexity of a large model with combined load cases is such that computer results cannot be readily assimilated. To obtain results with a reasonable amount of visibility, an orderly methodology was established. Each load case was individually analyzed for its contribution to the overall stress spectrum. Thus, individual loads could then be compared with hand computations and thereby establish a reasonable degree of credibility.

For instance, case 1 in Fig. 3, the 600°F limit temperature conditions when applied separately, provides the displacements shown in Fig. 5. This external growth in all directions was expected based on the hand calculations. The accuracy of the thermal growth in the computer results can be compared with a $\Delta l = L\alpha\Delta T$ calculation. A temperature increase of 600°F at a length of 600 in., produces a lockalloy skin growth calculated to be 3.38 in. The computer results show excellent correlation with the 3.35-in. growth indicated.

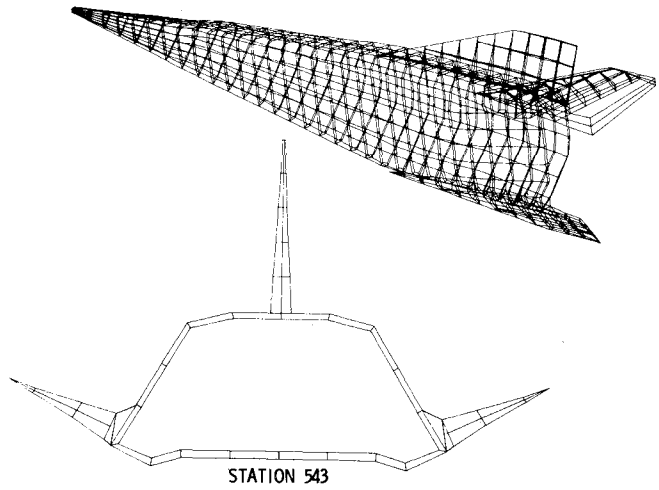

Fig. 6 Finite-element model of research airplane.

All the individual load cases were run in a similar manner. The load cases were then combined, and again logical steps were taken so that visibility of the results was not lost. When the vent loads, case 2, were combined with the thermal limit load, case 1, it is found that the inward vent load deflection on the lower surface was sufficient to counteract the outward thermal deflection so the net displacement was inward. This was opposite from what was expected and from what occurred on the upper half of the model. Further hand analysis verified this result. The deflection of the large flat base of the model due to the pressure load is sufficient to overcome the thermal growth.

When load case 3 (air loads) was run independently, large stresses and deflections were encountered. Since this air load is the balancing reaction for a 4g pullup, it will always be combined with load case 4, reducing the magnitude of the stresses. A summary of the maximum stress in each element from the individual load cases are shown in Table 1. From Table 1, it is evident that the thermal loads (cases 1 and 8) are the most significant individual design cases (cases 1, 2, 4, 8, and 13); in fact, the thermal stresses of case 8 nearly equal the ultimate stresses of case 10 that add the ultimate air loads to the limit thermal loads.

Finite-Element Model

A finite-element model was created to simulate the research airplane structure.[2] The model of Ref. 2 was refined and is shown in Fig. 6. The modifications include the addition of the vertical fin, bulkheads, longerons, intercostals, and midplane node points in the wing. This model complexity is essential to generate an adequate stiffness matrix for the analysis presented herein, particularly the thermal load cases.

All the primary structural components are modeled. This includes the external skins, longitudinal splices, inner and outer frame caps, frame web and flanges, and the web stiffeners. The current model consists of 803 node points, 621 of which are used to represent the fuselage shell structure.

A computer-generated plot of the entire model and a section through a frame station are shown in Fig. 6. There are approximately 2400 deg of freedom, 2161 rod elements simulating the splices, frame caps, stiffeners, and rigid mass connectors, 548 triangular panels simulating the contoured external skin, and 557 quadrilateral shear panels simulating frame, rib, and spar webs.

Design Concepts

Thermostructural design requires careful attention to the four basic variables affecting thermal stress. These are two material parameters (stiffness and thermal expansion coefficients), the temperature variations, and the relative stiffness

Table 1 Maximum element stresses for individual load cases

Load case	Case description	Structural elements: Inner cap 0.30 in.^{2} titanium	Outer cap 0.30 in.^{2} stainless steel	Longitudinal splice 0.125 in.^{2} stainless steel	Skin 0.15-0.75 in. Lockalloy
1	M9 low Q thermal	+ 94,608	−14,957	+ 6,406	−14,280
2	−1.0 psi vent	+ 20,694	− 2,065	+ 4,796	+ 4,115
3	+1.0 psi aerodynamic	+ 76,071	+13,808	−13,501	+12,370
4	4g inertia	− 30,992	− 3,415	+ 3,588	− 3,190
5	low Q limit	+108,400	−15,962	+ 9,379	−14,927
6	low Q ultimate	+122,116	−17,124	+13,507	−15,916
8	M9 high Q thermal	+120,376	−17,752	+ 6,034	−17,134
9	high Q limit	+120,285	−17,917	+ 5,942	−17,284
10	high Q ultimate	+120,239	−17,759	+ 5,979	−16,730
13	landing	+ 51,198	− 7,732	+ 4,185	− 9,563

of the expanding and restraining structures. The operating temperature of a heat-sink skin can be controlled by adding more material (heat capacity), but the amount of heat-sink material must be kept to a minimum in order to minimize weight.

The trade between structural surface temperature of the heat-sink and its weight was based on an operating temperature for Lockalloy of 600°F, where Lockalloy retains 75% of its room temperature structural properties. The heating rate and flight time are such that this 600°F skin temperature is reached very rapidly as seen in Fig. 7. As the outer skin is being heated, conduction, free convection, and radiation raise the temperature of the inner cap, but at a much lower rate than the outer skin. It is not until after the research aircraft has landed that the frame reaches a uniform temperature throughout its depth. In fact, after landing, the inner cap will be hotter than the exterior skin. The temperature difference reaches a maximum when the outer skin reaches its maximum temperature and is the source of an unavoidable thermal stress. This temperature difference would produce a stress of about 81,000 psi in an aluminum inner frame cap sized to support the air loads. This thermally induced stress is above the yield point of 7075-T6 aluminum. Since this stress level is unacceptable, thermostructural designs must be employed to reduce thermal stresses to an acceptable level.

Skin Splices

The skin splices run longitudinally and circumferentially, as shown in Fig. 4. The skin panels form a butt joint along each splice. This requires a width of about 2 in. to accommodate the minimum two rows of fasteners in the Lockalloy skin. These splices have large surface areas in contact with the inner skin surface. The temperature rise in these splices will lag only slightly behind the outer skin temperature as a result of low contact resistance provided by the high conductivity of the Lockalloy skin.[5]

The 600°F environment precludes the use of aluminum. Therefore, the likely candidates for this application are titanium and stainless steel. Figure 8 shows the skin and splice stresses present for both the titanium and stainless steel materials. The magnitude of the stresses in Figs. 8, 9, 10, and 12 is defined as the normal distance from the outer mold line of the fuselage to the curve. The titanium splices, Fig. 8a, are in tension both longitudinally and peripherally and the skins for this case are in biaxial compression. When stainless splices, Fig. 8b, are employed, the stresses are reduced.

There are several mechanisms that contribute to these thermal stresses. First, the skin is attempting to increase in size as in Fig. 1a, but the hoop frames and longitudinal splices tend to resist this growth as in Fig. 1b. Second, the overall nonlinear temperature profile (case 1 of Fig. 4) induces bending in the fuselage similar to Fig. 1c as the bottom tries to elongate more than the top and sides. As indicated in case 1 of Fig. 4, the bottom of the fuselage is 600°F, whereas the sides and top are at 575°F with a 25°F change in temperature occurring at the wing root or body chine. In the hoop direction, compression is expected in both the outer frame cap and skin, and tension is expected in the inner cap due to the resistance to thermal growth caused by the cold inner frame cap. Compression is evident in the skin and in the outer frame cap for the stainless steel splices (Fig. 8b) but the outer frame cap is in tension for the titanium splice case (Fig. 8a). This is due to the difference in α's (9.4×10^{-6} for Lockalloy and 5.7×10^{-6} for titanium) between the Lockalloy skin and titanium outer cap. Since the Lockalloy is attempting to expand more than the titanium and has more area, it stretches the outer cap placing it in tension while inducing more compression in the skin. A similar result occurs in the

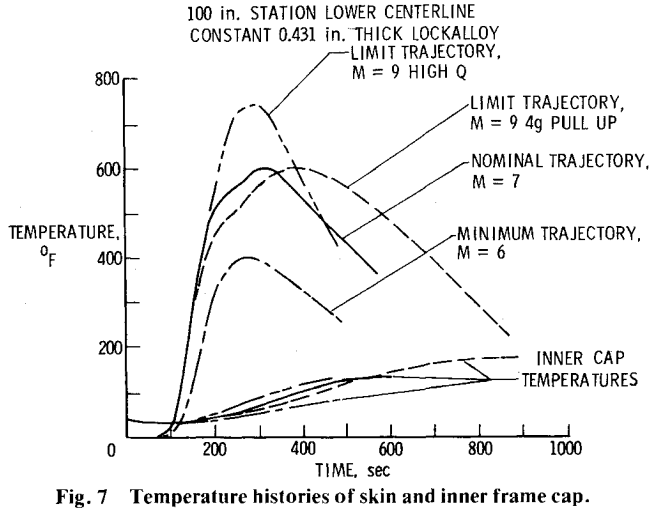

Fig. 7 Temperature histories of skin and inner frame cap.

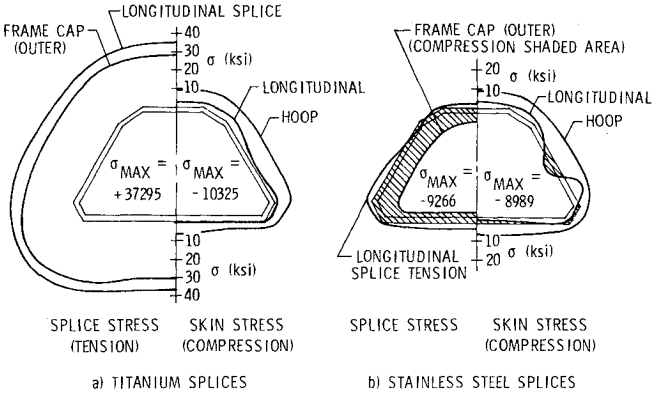

Fig. 8 Comparison of skin and splice stresses with alternate splice material.

longitudinal direction, where the small titanium splice is resisting growth of the large Lockalloy skin placing the skin in additional compression and the splice in tension. This is different to what is experienced with the stainless steel splices, where the induced fuselage bending governs, since there is virtually no difference in expansion coefficients (9.2×10^{-6} and 9.4×10^{-6}) between the stainless steel splices and the Lockalloy skins.

Both stainless steel and titanium are acceptable as splice material candidates in that both operate within their allowable stress at acceptable weight. However, Lockalloy has rather low yield strength, 22KSI at 600°F and 20 KSI at 750°F, and titanium tends to load the skin in compression, which is less desirable than tension because of buckling. The titanium splices would then increase the skin stress levels approximately 15% to about 11 KSI. Therefore, to avoid the unnecessary induced thermal stresses generated in the skin by the different α's of titanium and Lockalloy, stainless steel was selected for this study as the splice material. The maximum stresses generated in the stainless steel splices for the various load conditions are given in Table 1.

Frame Concepts

The fuselage frames are an area of great concern in the design of a heat-sink structure because they are essential to stabilize the shell and are a source of unavoidable thermal stress. As mentioned previously, the outer and inner caps of the frames are exposed to a severe temperature difference, which is responsible for the greatest thermal stresses. This frame temperature difference is not a function of vehicle configuration; therefore, the principal results of this study are applicable to other configurations. To minimize the thermal stresses in the frame, it is necessary to reduce the capability of the frame inner cap to resist the thermal growth of the external shell. Simultaneously, the frame must maintain acceptable stiffness and stress levels in its components to support the more conventional flight loads. Support of flight and thermal loads is accomplished by careful selection of the frame component sizes and materials to minimize the K factor, while simultaneously providing stiffness and bending strength for the flight loads.

Figure 9 shows the results of four separate frame designs. The Lockalloy skin and stainless steel skin splice form the effective outer cap for each of the cases. The four cases employ aluminum, E-glass epoxy, stainless steel, and titanium inner caps, respectively. The skin and inner cap stresses for the 600°F limit temperature condition at station 343 are compared for all four designs.

The low-cost aluminum inner cap, Fig. 9a, has a low modulus that would strain more than either the stainless or titanium for a given cap area. However, the stresses generated in a 0.6-in.^{2} inner cap exceed the 61 KSI yield strength of the aluminum alloy. An E-glass composite inner cap, Fig. 9b, h?s a much higher allowable and lower elastic modulus. This lowers the stresses in the skin and caps to acceptable values. However, the large deflections generated by the low stiffness of this concept are unacceptable when functional considerations such as tank clearance are evaluated.

The high-stiffness and high-strength stainless steel design, Fig. 9c, increases the stress level in both the skin and inner cap. This case has the maximum K value of the frame-skin concepts depicted and consequently has the least deflection, but the highest thermal stresses. The 119 KSI stress level is above the yield strength for the inner cap. Also, the 11 KSI compressive skin stress, while not near the yield strength, could pose local panel buckling problems in the low-heat-load (thin-skin) areas.

The fourth case, Fig. 9d, with titanium inner caps has two physical conditions that enhance its selection. Titanium has a relatively low elastic modulus, compared with Lockalloy or stainless steel, and a very high tensile strength. The skin stresses are reduced 25% below those with a stainless steel inner cap, and the 85 KSI inner cap stresses are about 60% of the titanium yield strength. Therefore, titanium was selected for the inner cap, frame, web, and stiffeners. It must be noted that these stresses are induced only by the thermal loads at 600°F, and other loads may be additive so that the high margins will be reduced when the flight loads are superimposed.

The maximum individual stresses in each type of fuselage element for each load case are summarized in Table 1. Cases 6 and 10 are ultimate load cases combining thermal loads with the ultimate pressure and flight loads. These stresses show no negative margins in any of the primary structural elements. The stresses shown represent an airframe consisting of Lockalloy skins and stainless steel splices and outer frame caps with titanium utilized for the frame webs, stiffeners, and inner caps.

With the primary structural design concept established, further investigation into discrete load conditions must be made since conventional design concepts for point loads can adversely affect a thermostructural design. Increasing the restraint factor K by adding structural components such as bulkheads, fittings, and longerons to react point loads can produce unacceptable results.

Bulkhead Concepts

Full- or partial-depth bulkheads will be a necessary part of any aircraft. They appear as firewalls, pressure bulkheads, and landing gear bays. To illustrate the impact of thermal loads on a bulkhead, the aft end of the cockpit was analyzed using several bulkhead concepts.

In Fig. 10, three bulkheads are compared. The first, shown in Fig. 10a, represents a cold 0.050-in.-thick aluminum

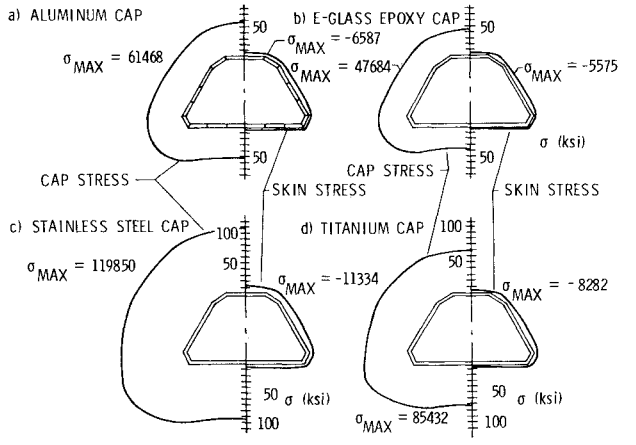

Fig. 9 Comparative frame stresses with alternate inner cap material.

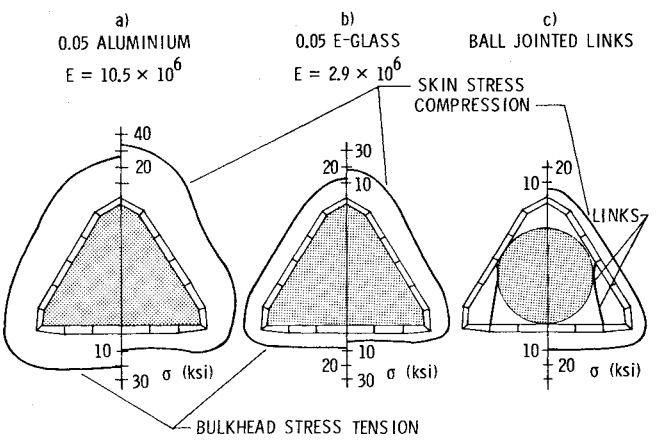

Fig. 10 Comparison of bulkhead stresses at 600 °F.

bulkhead resisting the expansion of the hot outer skin. The compressive hoop stresses generated in the skins (34,000 psi) exceed their yield strength. In Fig. 10b, an E-glass epoxy composite bulkhead, also 0.050 in. thick but with an elastic modulus of 2.9×10^6 lb/in.^{2}, is substituted for the aluminum. This reduces the skin stresses over 10 KSI; however, skin stresses are still near their yield point (20,000 psi) with only the 600°F thermal load. A minimum-gage aluminum bulkhead, 0.020 in. thick, will produce similar stresses to the 0.050 in. thick E-glass/epoxy bulkhead because of similar extensional stiffness. Since thinner materials are impractical from both deflection and minimum gage standpoints, conventional bulkhead concepts cannot satisfy the design requirements, and new concepts must be evaluated. In Fig. 10c, a pressure vessel with self-contained bulkheads is supported within the heat-sink structure by ball-jointed links. This concept offers no resistance to thermal growth. The inner cap stresses shown are generated only by the resistance of the basic ring frame resulting in maximum skin stresses of only about 7,000 psi. Simultaneously, the pressure vessel incurs no significant thermal loading.

Again, no loads other than the 600°F thermal cases are present in the analyses. However, these analyses show that conventional full-depth bulkheads cannot avoid high thermal loads due to their high K factor. Suspending the pressure compartment can avoid this thermal stress.

A full-depth bulkhead constructed as either a shallow cone with radial beads or as a flat structure with a peripheral slip joint could also be employed for firewalls and other walls with similar results. However, in such bulkhead designs, bellows seals, and reliable slip joints may require some development.

Intercostal or Fitting Concepts

Aircraft are subjected to more than uniformly distributed pressure loads. Very high local loads are encountered in areas such as landing gear supports, engine mounts, and other systems installations. Conventional aircraft design for these attachments consists of locally thickened skins, fittings (to beam the loads over several ring frames), and intercostals or heavier stringers to shear the loads into the skin.

This increase in the local stiffness in the internal structure will raise the relative resistance, K, to the thermal growth of the hot heat-sink skin. Figure 11 shows the results of two structural fitting concepts at 750°F. Both concepts depict a typical trunnion type support positioned on the longitudinal axis of the airplane. In both cases the exterior skin is at 750°F and the interior is maintained at 100°F (case 8 of Fig. 3). In Fig. 11a the stresses in the structural element due to a cold titanium conventional fitting are seen to be an order of magnitude higher than those in the ball-jointed truss of Fig. 11b. The ball-jointed truss concept, of equal weight, allows the exterior skin to move in all directions with no constraint, while retaining the trunnion centerline and providing suitable support for the applied loads.

Figure 11c shows the results of the point load case that simulates the landing loads. The temperatures have changed to 400°F for the outer skin and 200°F for the inner frame caps as shown in Fig. 7 after 700 s. The landing gear reaction is simulated by a 2.0g inertia load applied to the apex of two ball-jointed rods as described in Fig. 11c. The results show that the stresses in the Lockalloy skin structure in the vicinity of the landing gear are slightly higher than those in the 750°F limit thermal case. However, the stresses are very low and the maximum skin stress for this load case occurs at another location (Table 1), and is induced by the thermal load. In this landing gear area, as in most areas, the skin thickness required for the heat-sink function is sufficient to handle conventional loads once thermal stresses have been reduced.

Other cases were similarly examined including a 2.5g pullup with full propellant load, a 2g pylon attach load, the initial thrust, and the burnout thrust cases. None of these cases revealed any significant problem areas. This supports the premise that the thermal loads will be the primary structural design condition.

Temperature Variation Concepts

The exterior Lockalloy skin is sized to reach a uniform temperature during a specified nominal mission trajectory. Obviously this trajectory will not always be flown, and off-design trajectories will generate nonuniform temperatures over the skin surface. Additionally, local variations in heating caused by shock impingement or flow separation could produce similar temperature variations on the skin. In most cases, these variations will be small and will normally occur at lower peak temperatures than the limit case of 750°F, which is not expected to be achieved more than once in the life of the aircraft.

There are several planned experiments that will cause more severe temperature variations in the skin. For example, the propulsion experiment consists of a large engine attached to the lower fuselage, where the engine effectively shields the skin from the heating normally imposed on the covered surface. The resulting temperature differences will induce thermal loads that merit detailed investigation. The stresses induced by this internal constraint are shown in Figs. 12 and 13. Figure 12 depicts the stresses in the hoop direction for the skin, and Fig. 13 shows the stresses in the longitudinal direction for the skin. Figures 12a and 13a show the baseline

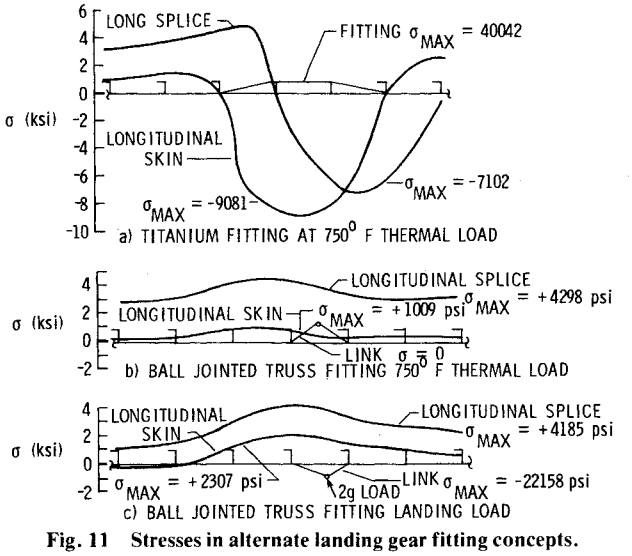

Fig. 11 Stresses in alternate landing gear fitting concepts.

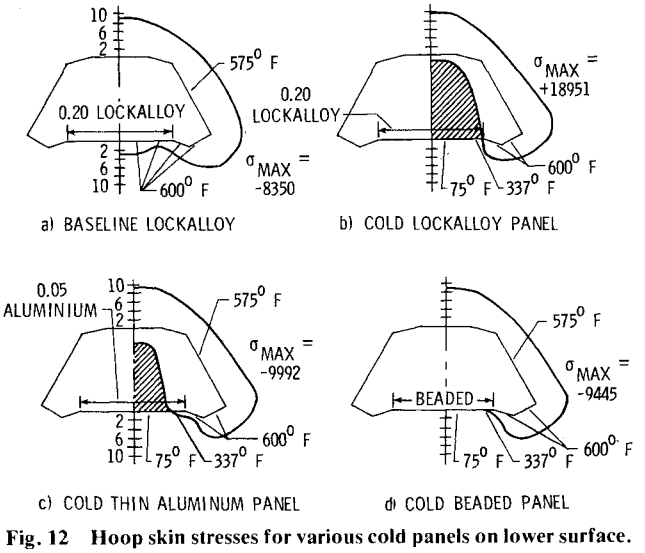

Fig. 12 Hoop skin stresses for various cold panels on lower surface.

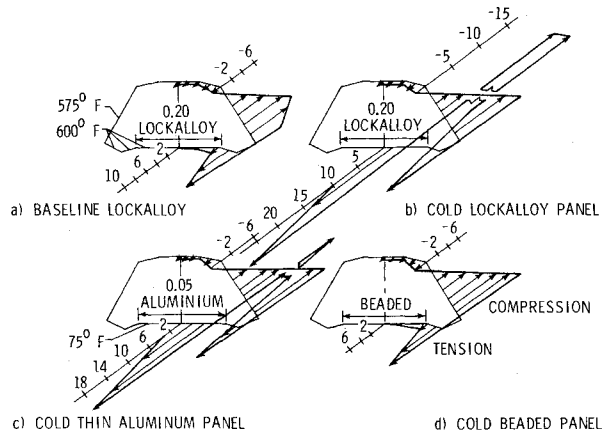

Fig. 13 Axial skin stresses for various cold panels on lower surface.

with the structure heated (per case 1 of Fig. 3) to 600°F across the bottom and 575°F on the sides and top. Figures 12b and 13b show the same structure subjected to a cold area on the bottom centerline. In Fig. 13b the axial thermal stresses are above 21 KSI at the cold interface where the research engine is installed. This stress is more than twice as high as the baseline and almost equal to the yield stress of Lockalloy. Increases in the local stresses are also evident in the hoop direction (Fig. 12b) where the skin stresses are about twice the baseline values due to the influence of the cold area. This indicates that the K factor for the small cold area is as significant as for the cold ring frame.

Several alternatives are available to alleviate these thermal stresses. First, the heat-sink skin thickness may be increased locally to make the temperature profile more linear, reducing the stresses.[6] However, this will adversely affect the structural weight. Alternate design concepts are shown in Figs. 12c, 12d, 13c, and 13d.

In Figs. 12c and 13c the 0.20-in.-thick heat-sink skin, covered by the scramjet, is replaced with an 0.05-in.-thick aluminum skin. The thin aluminum skin offers considerably less resistance, K, to the thermal growth of the airplane in both the longitudinal and hoop directions due to its reduced elastic modulus and area. This reduces the thermal stresses in the skins from 21 KSI in Fig. 13b to 9.4 KSI. However, the reduced stiffness of the lower body will cause slightly higher hoop bending stresses near the top of the frame.

In Figs. 12d and 13d, a beaded and slip-jointed skin replaces the cold Lockalloy skin. The maximum axial and hoop stresses in this case are about one-half that of the cold Lockalloy, Figs. 12b and 13b. Optimization of the frame and skin design may further reduce these values.

Again nonconventional design concepts are used to reduce the thermal stresses to an allowable level with no increase in weight. In fact, thin aluminum and beaded skins are substantially lighter than the baseline heat-sink concept.

Concluding Remarks

An in-depth structural analysis using a large finite-element model of a hypersonic research airplane has been conducted. The complexity of the analysis requires the use of a finite-element computer code such as SPAR to accurately calculate the component stresses in a reasonable amount of time. The results of this analysis show that thermal loads are the dominant forces in a heat-sink structural design and that most conventional aircraft structural concepts are unacceptable in a heat-sink design. However, with innovative design concepts and careful consideration of material and section properties, a viable heat sink structure is possible utilizing state-of-the-art materials and fabrication processes.

Several point design cases and thermal cases were analyzed to illustrate the problems with, and some solutions to, thermostructural design. The skin thickness required for the heat-sink with appropriate ring frames is sufficient to support both the thermal and air loads. Unlike conventional aircraft design, no additional structural provisions are required to support the internal loads. The stresses induced by unavoidable restraint of thermal growth are explained, and materials and section properties are selected for thermal compatibility to keep these stresses at acceptable levels. Additionally, innovative design concepts are shown that can alleviate thermal stresses. These include nonintegral pressure vessels, slip-jointed firewalls, fiberglass bulkheads, beaded webs and skins, as well as ball-jointed links utilized to suspend tanks, engines, landing gear, and the crew compartment. These concepts are used to minimize the restraint to the thermal growth of the outer surface while supporting the various internal components. A number of point design cases (landing, launch, pullup, and burnout) were examined, and show that no significant structural problems are inherent in the proposed concepts. In fact, once the structure has been designed to alleviate thermal stresses, the conventional loads are readily supported with the skins sized by the heat load requirements.

References

[1] Hearth, D. P. and Preyss, A. E., "Hypersonic Technology – Approach to an Expanded Program" *Aeronautics and Astronautics*, Vol. 14, Dec. 1976, pp. 20-37.

[2] Jackson, L. R. and Taylor, A. H., "A Structural Design for a Hypersonic Research Airplane," AIAA Paper 76-906, Dallas, Texas, Sept. 1976.

[3] Duba, R. J., Haramis, A. C., Marks, R. F., Payne, L., and Sessing, R. C., "YF-12 Lockalloy Ventral Fin Program Final Report," Vol. 1, Lockheed-California Company, Advanced Development Projects, CR-144971, Jan. 1976, NASA.

[4] Whetstone, W. D., *SPAR Reference Manual*, NASA CR-120504, 1975.

[5] Minges, M. L., "Thermal Contact Resistance," AFML-TR-65-375, April 1966.

[6] Combs, H. G., et al., "Configuration Development Study of the X-24C Hypersonic Research Airplane-Phase III," Lockheed-California Company, Advanced Development Projects, NASA CR-145103, 1977.